Nonlinear Behaviors of Second-order Digital Filters with Two's Complement Arithmetic

Bingo Wing-Kuen Ling
Department of Electronic and
Information Engineering,
HKPU, H.K.
(852) 2766 4094

bingo@eie.polyu.edu.hk

Charlotte Yuk-Fan Ho
IEEE Member
Department of Electronic and
Information Engineering,
HKPU, H.K.
(852) 2766 4094

enhyfan@eie.polyu.edu.hk

Peter Kwong-Shun Tam
IEEE Member
Department of Electronic and
Information Engineering,
HKPU, H.K.
(852) 2766 4094

enptam@polyu.edu.hk

ABSTRACT

The main contribution of our work is the further exploration of some novel and counter-intuitive results on nonlinear behaviors of digital filters and provides some analytical analysis for the account of our partial results. The main implications of our results is: (1) one can select initial conditions and design the filter parameters so that chaotic behaviors can be avoided; (2) one can also select the parameters to generate chaos for certain applications, such as chaotic communications, encryption and decryption, fractal coding, etc; (3) we can find out the filter parameters when random-like chaotic patterns exhibited in some local regions on the phase plane by the Shannon entropies.

Keywords

Chaos, digital filter, two's complement arithmetic.

1. INTRODUCTION

The second-order digital filter is a fundamental building block of the cascade and parallel realizations of digital filters, which have found many applications in industry. The simplest configuration for realizing the second-order filter is the direct form realization which uses the least number of multipliers and adders. It is commonly implemented in hardware using a two's complement arithmetic for the addition operation. When overflow occurs, a flag is set and error messages may be prompted. If we neglect the flag or warnings and continue the process, chaotic phenomena occurs [1]-[10].

Some papers have explored the chaotic behaviors of digital filters when they are operating at the unstable region [8], [9]. In section III-V, we will provide some new results in the form of counter-intuitive phenomena, such as the linear and periodic behaviors of digital filters when they are operating at the unstable region, as well as the chaotic behaviors of digital filters when they are operating at the stable region.

In section VI, the statistical property of the symbolic sequences and state variables are investigated, and some interesting results are reported.

Most of the existing literature on the analysis of second-order

digital filters with two's complement arithmetic study only the autonomous response and assume that the filters are operating at the marginally stable region [1], [4], [6], [7], [10]. In section VII and VIII, we will extend some of their results to the forced response cases, such as the step response case and the sinusoidal response case.

The existing literature covers the analysis of a direct form third-order digital filter with two's complement arithmetic [3]. In section IX, some of our results on the cascade and parallel forms will be covered.

Some papers study the effects of other nonlinearities, such as saturation type nonlinearity [2] and quantization type nonlinearity [5]. For these nonlinearities, we will also provide further insight on the behaviors of the filters in section IX.

Besides the discovery of some novel and counter-intuitive results on the behaviors of digital filters discussed in the abstract, another main contribution of our work is to provide some analytical results on the behaviors of digital filters. In section III, we provide a relationship between the properties of symbolic sequences and the behaviors of various types of trajectories (including the case when the trajectory converges to some fixed points not locating at the origin, and the cases when limit cycle and chaotic fractal patterns occur) when the digital filter is operating at the stable region. The initial conditions for the corresponding trajectories are also given. In section IV, when the digital filter is operating at the unstable region, we provide the condition for which overflow does not occur and the trajectory converges to some fixed points or periodic orbits. The stability of the trajectories with respect to the initial conditions and filter parameters are also discussed. In section VII and VIII, we also extend the analysis of autonomous system to the forced response cases. For the step response case, an appropriate affine transformation is developed to relate the step response behaviors to some corresponding autonomous response behaviors. Based on the transformation, a set of necessary and sufficient conditions is derived to relate the trajectory equations, symbolic sequences and the set of initial conditions for various types of trajectories. For the sinusoidal response case, a frequency-domain technique is employed to derive the sets of initial conditions and the necessary conditions on the filter parameters. The periodicity of the symbolic sequences is used for the characterization of the

overflow, and the set of initial conditions for overflow is figured out.

The main implications of our results is: (1) one can select initial conditions and design the filter parameters so that chaotic behaviors can be avoided; (2) one can also select the parameters to generate chaos for certain applications, such as chaotic communications, encryption and decryption, fractal coding, etc.

2. SYSTEM DESCRIPTION

Assume that a second-order digital filter with two's complement arithmetic is realized in direct form, as shown in figure 1. The state space model of the overall system can be represented as follows:

$$\mathbf{x}(k+1) \equiv \begin{bmatrix} x_1(k+1) \\ x_2(k+1) \end{bmatrix} = \begin{bmatrix} x_2(k) \\ f(b \cdot x_1(k) + a \cdot x_2(k) + u(k)) \end{bmatrix} \text{ for } k \geq 0 \quad (1)$$

where a and b are the filter parameters; $x_1(k)$ and $x_2(k)$ are the state variables; $u(k)$ is the input of the digital filter; and f is the nonlinearity due to the use of two's complement arithmetic.

The nonlinearity f can be modeled as:

$$f(v) = v - 2 \cdot n \text{ such that } 2 \cdot n - 1 \leq v < 2 \cdot n + 1 \text{ and } n \in Z \quad (2)$$

Hence, the state space model of the overall system can be represented as:

$$\mathbf{x}(k+1) = \begin{bmatrix} x_2(k) \\ b \cdot x_1(k) + a \cdot x_2(k) + u(k) + 2 \cdot s(k) \end{bmatrix} \quad (3)$$

$$= \mathbf{A} \cdot \mathbf{x}(k) + \mathbf{B} \cdot u(k) + \begin{bmatrix} 0 \\ 2 \end{bmatrix} \cdot s(k) \text{ for } k \geq 0 \quad (4)$$

where $\begin{bmatrix} x_1(k) \\ x_2(k) \end{bmatrix} \in I^2 \equiv \left\{ \begin{bmatrix} x_1(k) \\ x_2(k) \end{bmatrix} : -1 \leq x_1(k) < 1, -1 \leq x_2(k) < 1 \right\}$ for $k \geq 0$ (5)

$$\mathbf{A} \equiv \begin{bmatrix} 0 & 1 \\ b & a \end{bmatrix} \quad (6)$$

$$\mathbf{B} \equiv \begin{bmatrix} 0 \\ 1 \end{bmatrix} \quad (7)$$

and $s(k) \in \{-m, \cdots, -1, 0, 1, \cdots, m\}$ for $k \geq 0$ (8)

in which m is the minimum integer satisfying

$$-2 \cdot m - 1 \leq b \cdot x_1(k) + a \cdot x_2(k) + u(k) < 2 \cdot m + 1 \text{ for } k \geq 0 \quad (9)$$

3. CHAOTIC BEHAVIORS IN STABLE SECOND-ORDER DIGITAL FILTERS

When the eigenvalues of $\mathbf{A}$ are inside the unit circle, one may expect that the state trajectory of the autonomous system will converge to the origin of the phase plane. However, this is not true. In fact, by defining:

$$b = -r^2 \quad (10)$$

and

$$a = 2 \cdot r \cdot \cos \theta \quad (11)$$

where

$$\theta \in \Re \quad (12)$$

and

$$0 < r < 1 \quad (13)$$

we have found that there are four types of trajectories. The type I trajectory can be defined as the one which corresponds to the 'no overflow' case, that is, $s(k) = 0$ for $\forall k \geq 0$. The trajectory will converge to the origin and the set of initial conditions is a polygon containing the origin. The type II trajectory can be defined as the one which corresponds to the case when the symbolic sequences are non-zero constant integers, that is, $s(k) = s_0 \neq 0$ for $\forall k \geq 0$. The trajectory will converge to the fixed points $\mathbf{x}^* = \dfrac{2 \cdot s_0}{\sin \theta \cdot (1 - 2 \cdot r \cdot \cos \theta + r^2)} \cdot \begin{bmatrix} 1 \\ 1 \end{bmatrix}$ (different values of s_0 corresponds to different fixed points), and the set of initial conditions is a set of polygons with each polygon containing a fixed point. The type III trajectory can be defined as the one which corresponds to the case when the symbolic sequences are periodic, that is, $\exists M \in Z^+ \setminus \{1\}$ such that $s(k) = s(k+M)$ for $\forall k \geq k_0$. The trajectory will converge to a periodic sequence $\{\mathbf{x}_0^*, \mathbf{x}_1^*, \cdots \mathbf{x}_{M-1}^*\}$, where

$$\mathbf{T} = \begin{bmatrix} \dfrac{1}{\sqrt{r}} \cdot e^{-\frac{j \cdot \theta}{2}} & \dfrac{1}{\sqrt{r}} \cdot e^{\frac{j \cdot \theta}{2}} \\ \sqrt{r} \cdot e^{\frac{j \cdot \theta}{2}} & \sqrt{r} \cdot e^{-\frac{j \cdot \theta}{2}} \end{bmatrix} \quad (14)$$

$$\mathbf{x}_0^* = \sum_{n=0}^{M-1} \mathbf{T} \cdot \begin{bmatrix} \dfrac{r^{M-1-n} \cdot e^{j(M-1-n)\theta}}{1 - r^M \cdot e^{jM\theta}} & 0 \\ 0 & \dfrac{r^{M-1-n} \cdot e^{-j(M-1-n)\theta}}{1 - r^M \cdot e^{-jM\theta}} \end{bmatrix} \cdot \mathbf{T}^{-1} \cdot \begin{bmatrix} 0 \\ 2 \end{bmatrix} \cdot s(k_0 + n) \quad (15)$$

$$\mathbf{x}_n^* = \mathbf{A}^n \cdot \mathbf{x}_0^* + \sum_{m=0}^{n-1} \mathbf{A}^{n-1-m} \cdot \begin{bmatrix} 0 \\ 2 \end{bmatrix} \cdot s(k_0 + m) \text{ for } n = 1, 2, \cdots, M-1 \quad (16)$$

and the set of initial conditions is sets of polygons. The type IV trajectory can be defined as the one which corresponds to the case when the symbolic sequences are aperiodic. The trajectory exhibits chaotic polygonal fractal patterns, and the set of initial conditions are also of polygonal fractal patterns.

The above result provides relationships between the properties of symbolic sequences and the behaviors of various types of trajectories including the case when the trajectory converges to some fixed points not locating at the origin, and the cases when limit cycle and chaotic fractal patterns occurs. The set of initial conditions corresponding to those trajectories also provides useful information, such as one can determine the behaviors of the system precisely for any arbitrary initial conditions and filter parameters in the stable region. The mathematical analysis can be found in [16], and some simulation results are shown in figure 2.

4. PERIODIC BEHAVIORS IN UNSTABLE SECOND-ORDER DIGITAL FILTERS

When $b = a+1$ or $b = -a+1$ and an eigenvalue of $\mathbf{A}$ is outside the unit circle, one may expect that overflow will always occur and the state trajectory will be chaotic or aperiodic for the autonomous response. However, we have found that overflow may not occur and the state trajectories may converge to some fixed points or periodic orbits. The results are summarized in the following Lemmas:

Lemma 1:

For $b = a+1$, *if* $\exists M \in Z^+$ such that $\begin{bmatrix} x_1(k) \\ x_2(k) \end{bmatrix} = \begin{bmatrix} x_1(k+M) \\ x_2(k+M) \end{bmatrix}$ for

$k \geq k_0$, *then*

$$(x_1(0) + x_2(0)) \cdot ((a+1)^M - 1) + 2 \cdot (2 \cdot (a+1)^M - 1) \cdot \sum_{j=0}^{k_0-1} \frac{s(j)}{(a+1)^{j+1}} + $$

$$2 \cdot (a+1)^M \cdot \sum_{j=k_0}^{k_0+M-1} \frac{s(j)}{(a+1)^{j+1}} = 0$$

Lemma 2:

For $b = -a+1$, *if* $\exists M \in Z^+$ such that $\begin{bmatrix} x_1(k) \\ x_2(k) \end{bmatrix} = \begin{bmatrix} x_1(k+M) \\ x_2(k+M) \end{bmatrix}$ for

$k \geq k_0$, *then*

$$\left(1 - (a-1)^M\right) \cdot \left(x_1(0) - x_2(0) - 2 \cdot \sum_{j=0}^{k_0-1} \frac{s(j)}{(a-1)^{j+1}}\right) + 2 \cdot \sum_{j=k_0}^{k_0+M-1} (a+1)^{M-j-1} \cdot s(j) = 0$$
.

Lemma 3:

For $b = a+1$ and $|a+1| > 1$, $s(k) = 0$ for $k \geq k_0$ *if and only if* $\exists k_0 \in Z^+ \cup \{0\}$ such that $x_1(k_0) = -x_2(k_0)$.

Lemma 4:

For $b = a+1$ and a being an odd integer, $\exists k_0 \in Z^+ \cup \{0\}$ such that $x_1(k_0) = x_2(k_0) = -1$ *if and only if* $s(k) = a$ and $\begin{bmatrix} x_1(k) \\ x_2(k) \end{bmatrix} = \begin{bmatrix} x_1(k_0) \\ x_2(k_0) \end{bmatrix}$ for $k \geq k_0$.

Lemma 5:

For $b = -a+1$ and $|a-1| > 1$, $s(k) = 0$ for $k \geq k_0$ *if and only if* $\exists k_0 \in Z^+ \cup \{0\}$ such that $x_1(k_0) = x_2(k_0)$.

Lemma 6:

For $b = -a+1$ and a being an odd integer, there does not exist $k_0 \in Z^+$ such that $s(k) = a$ for $k \geq k_0$.

The proofs of the above Lemmas and the stability analysis can be found in [15]. Some simulation results are shown in figure 3.

Since one of the eigenvalues is unstable, one may expect that a very small deviation from the initial condition or filter parameter will produce a very different trajectory pattern. However, a counter-intuitive result is found that fixed points or periodic orbits exists and are stable if a is an odd integer and $b = a+1$ or $b = -a+1$ for all the initial conditions in I^2. That is, an arbitrary initial condition will still converge either to a fixed point or a periodic orbit. However, it is not true for the filter parameters. When a deviates from an odd integer a little bit, the state does not converge neither to a fixed point nor a periodic orbit.

5. NEW TRAJECTORY PATTERN IN UNSTABLE SECOND-ORDER DIGITAL FILTERS

We have reported in section IV that the trajectory is periodic for some special initial conditions when $b = a+1$ or $b = -a+1$ and an eigenvalue of $\mathbf{A}$ is outside the unit circle. Are these results valid for any arbitrary initial conditions and other filter parameters on the extended boundaries of the stability triangle, such as $b = -1$? If yes, what are the trajectory patterns exhibited on the phase plane for those filter parameters? The answers are summarized in the following observations:

Observation 1.

If:

(i) $b = -1$ and $|a| = 2^n + \frac{1}{2^n}$ where $n \in \mathbf{Z} \setminus \{0\}$, or

(ii) $b = a+1$ and $|b| > 1$ and a is an odd number, or

(iii) $\quad b = -a+1$ and $|b| > 1$ and a is an odd number,

then $\exists k_0 \in \mathbf{Z}^+ \cup \{0\}$ and $\exists M \in \mathbf{Z}^+$ such that $\mathbf{x}(k+M) \approx \mathbf{x}(k)$ for $\forall k \geq k_0$ and $\forall \mathbf{x}(0) \in I^2$.

Observation 2.

If $b = -1$ and $|a| = 2^n + \frac{1}{2^n}$ where $n \in \{-3,-2,-1,1,2,3,4\}$, then a new trajectory pattern, which looks like a rotated letter 'X', is exhibited on the phase plane, no matter what the values of the initial conditions are. The center of the rotated letter is located at the origin, and the slopes of the 'straight lines' of the rotated letter 'X' are equal to the values of the pole locations.

More discussions can be found in [12] and some simulation results are shown in figure 4 and figure 5, respectively.

6. DETECTION OF SPECIAL TRAJECTORY PATTERNS

Since there are some special trajectory patterns exhibited on the phase plane when the eigenvalues of $\mathbf{A}$ are outside the unit circle, are there any methods to detect those special trajectory patterns on the phase plane? We have found that when both the eigenvalues of $\mathbf{A}$ are outside the unit circle, the Shannon entropies of the state variables are independent of the initial conditions and the filter parameters, except for some special values of filter parameters, as shown in figure 6. At those special values of the filter parameters, the Shannon entropies of the state variables are relatively small. The state trajectories corresponding to those filter parameters either exhibit random-like chaotic behaviors in some local regions or converge to fixed

points on the phase plane, as shown in figure 7. Hence, by measuring the Shannon entropies of the state variables, those special state trajectory patterns can be detected.

For completeness, we extend the investigation to the case when the eigenvalues of $\mathbf{A}$ are complex and not outside the unit circle (stable one or the marginally stable one). We have found that the Shannon entropies of the symbolic sequences for the type II trajectories may be higher than that for the type III trajectories, even though the symbolic sequences of the type II trajectories are periodic and correspond to limit cycle behaviors, while that of the type III trajectories are aperiodic and correspond to chaotic behaviors. Some simulation results are shown in figure 8. For more information, the readers may refer to [13].

7. STEP RESPONSE OF SECOND-ORDER DIGITAL FILTERS

Up to now, the discussions are based on the autonomous response case. What are the results for the forced response cases, such as the step response case? Do they still exhibit the same types of trajectories similar to those of the autonomous response case? If so, what are the differences between the step response and the autonomous response? Does overflow occur for the type I trajectory? Do there always exist some initial conditions such that the digital filters exhibit the type I trajectory for small step input? Can we say that when the input step size is large, there does not exist any initial conditions for the system to exhibit the type I trajectory? Moreover, can the step response behaviors be related to some corresponding autonomous response behaviors by means of an appropriate affine transformation in the presence of the overflow nonlinearity? To address the above problems, let:

$$u(k) = c, \text{ for } k \geq 0 \text{ and } c \in \Re \tag{17}$$

Define:

$$\cos\theta \equiv \frac{a}{2} \tag{18}$$

$$\mathbf{T} \equiv \begin{bmatrix} 1 & 0 \\ \cos\theta & \sin\theta \end{bmatrix} \tag{19}$$

$$\widehat{\mathbf{A}} \equiv \begin{bmatrix} \cos\theta & \sin\theta \\ -\sin\theta & \cos\theta \end{bmatrix} \tag{20}$$

$$\mathbf{x}^* \equiv \frac{c}{2-a} \cdot \begin{bmatrix} 1 \\ 1 \end{bmatrix} \tag{21}$$

$$s_0 \equiv s(0) \tag{22}$$

and

$$\widehat{\mathbf{x}}(k) \equiv \begin{bmatrix} \hat{x}_1(k) \\ \hat{x}_2(k) \end{bmatrix} \equiv \mathbf{T}^{-1} \cdot \left(\mathbf{x}(k) - \frac{c + 2 \cdot s_0}{2 - a} \cdot \begin{bmatrix} 1 \\ 1 \end{bmatrix} \right) \tag{23}$$

Then we have the following Lemmas:

Lemma 7:

The following three statements are equivalents:

(i) $\widehat{\mathbf{x}}(k+1) = \widehat{\mathbf{A}} \cdot \widehat{\mathbf{x}}(k)$ for $k \geq 0$.

(ii) $s(k) = s_0$ for $k \geq 0$.

(iii) $\mathbf{x}(0) \in \left\{ \mathbf{x}(0) : \left\| \mathbf{T}^{-1} \cdot \left(\mathbf{x}(0) - \frac{c + 2 \cdot s_0}{2 - a} \cdot \begin{bmatrix} 1 \\ 1 \end{bmatrix} \right) \right\| \leq 1 - \frac{|c + 2 \cdot s_0|}{2 - a} \right\}$.

The proof of Lemma 7 can be found in [18].

Lemma (7i) implies that there is a single ellipse exhibited on the phase plane. This result is the same as that of the autonomous response case. Hence, this result corresponds to the type I trajectory. However, the center of the ellipse is located at $\frac{c + 2 \cdot s_0}{2 - a} \begin{bmatrix} 1 \\ 1 \end{bmatrix}$, instead of at the origin for the autonomous response. It is interesting to note that when $s_0 \neq 0$, overflow occurs. Hence, overflow may occur even for the type I trajectory.

According to Lemma (7iii), the set of initial conditions for the type I trajectory is elliptic in shape, with the center being the same as that of the trajectory. The size of the elliptical region of the set of initial conditions depend on the value of $1 - \frac{|c + 2 \cdot s_0|}{2 - a}$, which should of course be greater than zero. This implies that $2 - a \geq |c + 2 \cdot s_0|$. For a given s_0, the possible values of a and c are in a translated triangle. Hence, the parameter space also includes the points with large values of c. It means that the system will also give the type I trajectory even if the input step size is so large that overflow always occurs. On the other hand, there are some values of a and c which are not in the parameter space. This region includes the case for very small values of c. This implies that the corresponding system can never give the type I trajectory even though the input step size tends to a value very close to zero, no matter what the initial conditions are.

Suppose θ is not an integer multiple of π. Then

$$|\mathbf{I} - \mathbf{A}^M| \neq 0, \text{ and so } (\mathbf{I} - \mathbf{A}^M)^{-1} \text{ exists.} \tag{24}$$

Define:

$$\mathbf{x}_0^* \equiv (\mathbf{I} - \mathbf{A}^M)^{-1} \cdot \left(\sum_{j=0}^{M-1} \mathbf{A}^j \cdot \mathbf{B} \cdot c + \sum_{j=0}^{M-1} \mathbf{A}^{M-1-j} \cdot \begin{bmatrix} 0 \\ 2 \end{bmatrix} \cdot s(j) \right) \tag{25}$$

$$\mathbf{x}_{i+1}^* \equiv \mathbf{A} \cdot x_i^* + \mathbf{B} \cdot c + \begin{bmatrix} 0 \\ 2 \end{bmatrix} \cdot s(i) \text{ for } i = 0,1,\cdots,M-2 \tag{26}$$

$$\widehat{\mathbf{x}}_i(k) = \mathbf{T}^{-1} \cdot \left(\mathbf{x}(k \cdot M + i) - \mathbf{x}_i^* \right) \text{ for } k \geq 0 \text{ and } i = 0,1,\cdots,M-1 \tag{27}$$

Lemma 8:

The following three statements are equivalents:

(i) $\widehat{\mathbf{x}}_i(k+1) = \widehat{\mathbf{A}}^M \cdot \widehat{\mathbf{x}}_i(k)$ for $k \geq 0$ and $i = 0,1,\cdots,M-1$.

(ii) $\exists M$ such that $s(M \cdot k + i) = s(i)$ for $k \geq 0$ and $i = 0,1,\cdots,M-1$.

(iii) $\mathbf{x}(0) \in \left\{ \mathbf{x}(0) : \left\| \mathbf{T}^{-1} \cdot \left(\mathbf{x}(i) - \mathbf{x}_i^* \right) \right\| \leq 1 - \left\| \mathbf{x}_i^* \right\|_\infty \right\}$ for $i = 0,1,\cdots,M-1$.

The proof of Lemma 8 can be found in [18].

Lemma (8i) implies that there are M ellipses exhibited on the phase plane. This result is the same as that of the autonomous

response. Hence, this result corresponds to the type II trajectory. The center of these ellipses are located at $\mathbf{x}_i^*$, for $i = 0,1,\cdots,M-1$.

It is interesting to note that even the digital filters are nonlinear, the step response behaviors can still be related to some corresponding autonomous response behaviors by means of an appropriate affine transformation. This is in general not true for arbitrary nonlinear functions.

Lemma 8 implies that the set of initial conditions corresponding to the type II trajectory are some rotated and translated elliptical regions. For each periodic symbolic sequence $s(M \cdot k + i) = s(i)$, for $i = 0,\cdots,M-1$, we have a corresponding single rotated and translated ellipse with center at $\mathbf{x}_i^*$. The centers are the same as that of the trajectory described in Lemma 7. Hence, comparing to that of the autonomous response case, the centers are shifted to different positions, and the shifts depend on the filter parameter a, input step size, and the periodicity of the symbolic sequences. By transforming these ellipses to circles, the radii of these circles are $1 - \left\| \mathbf{x}_i^* \right\|_\infty$.

Based on extensive simulations, we observe that the system may give an elliptical fractal pattern of trajectory if the system does not give the type I or type II trajectories. Let:

$$D_M = \left\{ \mathbf{x}(0): \left\| \mathbf{T}^{-1} \cdot \left(\mathbf{x}(i) - \mathbf{x}_i^* \right) \right\| \le 1 - \left\| \mathbf{x}_i^* \right\| \text{ and } s(i) = s(i+M) \text{ for } M \in Z \setminus \{0\} \right\}$$
(28)

and

$$D = I^2 \setminus \bigcap_{\forall M} D_M$$
(29)

Then the set of initial conditions that may give the type III trajectory is D.

One main contribution of our results is to extend the necessary condition relating the symbolic sequences and trajectory behaviors in [1] to the necessary and sufficient conditions. We also explore the necessary and sufficient conditions of relating the trajectory behaviors and the set of initial conditions. The detail analysis and description can be found in [18]. Some simulation result is shown in figure 9.

8. SINUSOIDAL RESPONSE OF SECOND-ORDER DIGITAL FILTERS

The step response case is discussed in section VII. How about the sinusoidal response case? It is found that the visual appearance of the trajectory for the sinusoidal response case is much richer than that of the autonomous and step response cases, as shown in figure 10. When overflow does not occur, several ellipses may be exhibited on the phase plane (as shown in figure 10a), which corresponds to the overflow case in the autonomous and step response cases. Hence, the occurrence of overflow cannot be studied by examining the visual appearances of the trajectories. Instead, the periodicity of the symbolic sequences is employed for the characterization of the overflow. The results are summarized as the following Lemmas:

Lemma 9:

Let:

$$u(k) = c \cdot \sin(\theta \cdot k) \cdot v(k)$$
(30)

where

$$c \in \Re \setminus \{0\}$$
(31)

$$\theta \in \Re \setminus \{k \cdot \pi : k \in Z\}$$
(32)

and

$$v(k) = \begin{cases} 1 & k \ge 0 \\ 0 & \text{otherwise} \end{cases}$$
(33)

Define:

$$\cos \Omega \equiv \frac{a}{2}$$
(34)

$$\mathbf{T}_\Omega \equiv \begin{bmatrix} 1 & 0 \\ \cos \Omega & \sin \Omega \end{bmatrix}$$
(35)

$$\mathbf{T}_\theta \equiv \begin{bmatrix} 1 & 0 \\ \cos \theta & \sin \theta \end{bmatrix}$$
(36)

$$\widehat{\mathbf{A}}_\Omega \equiv \begin{bmatrix} \cos \Omega & \sin \Omega \\ -\sin \Omega & \cos \Omega \end{bmatrix}$$
(37)

$$\widehat{\mathbf{A}}_\theta \equiv \begin{bmatrix} \cos \theta & \sin \theta \\ -\sin \theta & \cos \theta \end{bmatrix}$$
(38)

and

$$\mathbf{x}_1^* \equiv \frac{c \cdot \sin \theta}{2 \cdot \cos \theta - a} \cdot \begin{bmatrix} 1 \\ 0 \end{bmatrix}$$
(39)

If $s(k) = 0$ for $\forall k \in Z$, then:

(i) $\mathbf{x}(k) = \mathbf{T}_\Omega \cdot \widehat{\mathbf{A}}_\Omega^{\ k} \cdot \mathbf{T}_\Omega^{-1} \cdot \left(\mathbf{x}(0) + \mathbf{x}_1^* \right) - \mathbf{T}_\theta \cdot \widehat{\mathbf{A}}_\theta^{\ k} \cdot \mathbf{T}_\theta^{-1} \cdot \mathbf{x}_1^*$ for $k \ge 1$.

(ii) $\left\{ \mathbf{x}(0): \left\| \mathbf{T}_\Omega^{-1} \cdot \left(\mathbf{x}(0) + \mathbf{x}_1^* \right) \right\| \le 1 - \left\| \mathbf{T}_\theta^{-1} \cdot \mathbf{x}_1^* \right\| \right\}$.

(iii) $\dfrac{|c|}{2} \le \left| \cos \Omega - \cos \theta \right|$.

The proof of Lemma 9 can be found in [19].

Since $\mathbf{x}(k)$ is the superposition of two signals with different frequencies, this gives a rich set of trajectory patterns on the phase portrait. According to Lemma (9ii), the set of initial conditions can be represented as an elliptical region in the phase portrait diagram. The center of the ellipse is located at $-\mathbf{x}_1^*$ and the size of the ellipse depends on $1 - \left\| \mathbf{T}_\theta^{-1} \cdot \mathbf{x}_1^* \right\|$. If Lemma (9iii) is not satisfied, overflow has to occur no matter what the initial conditions are. For example, if $\theta = 2 \cdot \pi \cdot m \pm \Omega$, then c has to be zero. Therefore, overflow will occur no matter what the initial conditions are, even when a very small signal ($c \to 0$, where $|c| > 0$) is applied to the system. This phenomenon can be understood by considering the resonance behavior.

Lemma 10:

If $\exists M \in Z \setminus \{0\}$ such that $s(k) = s(k + M)$ for $\forall k \in Z$, then:

$\exists a_p, b_p \in \Re$ for $p = 0, 1, \cdots, M - 1$ such that

$$s(k) = \sum_{p=0}^{M-1} a_p \cdot \sin(p \cdot \omega \cdot k) + b_p \cdot \cos(p \cdot \omega \cdot k) \text{ for } k \geq 0 \qquad (40)$$

where

$$\omega = \frac{2 \cdot \pi}{M} \qquad (41)$$

Let:

$$\mathbf{x}_{1,p}^* = \frac{a_p \cdot \sin(p \cdot \omega)}{\cos(p \cdot \omega) - \cos\Omega} \cdot \begin{bmatrix} 1 \\ 0 \end{bmatrix} \qquad (42)$$

$$\mathbf{x}_{2,p}^* = \frac{b_p}{\cos(p \cdot \omega) - \cos\Omega} \cdot \begin{bmatrix} \cos(p \cdot \omega) \\ 1 \end{bmatrix} \qquad (43)$$

$$\mathbf{T}_{p \cdot \omega} = \begin{bmatrix} 1 & 0 \\ \cos(p \cdot \omega) & \sin(p \cdot \omega) \end{bmatrix} \qquad (44)$$

$$\widehat{\mathbf{A}}_{p \cdot \omega} = \begin{bmatrix} \cos(p \cdot \omega) & \sin(p \cdot \omega) \\ -\sin(p \cdot \omega) & \cos(p \cdot \omega) \end{bmatrix} \qquad (45)$$

$$\mathbf{x}_2^* = \frac{b_0}{1 - \cos\Omega} \cdot \begin{bmatrix} 1 \\ 1 \end{bmatrix} \qquad (46)$$

and

$$\mathbf{x}_3^* = \frac{b_{\frac{M}{2}}}{1 + \cos\Omega} \cdot \begin{bmatrix} -1 \\ 1 \end{bmatrix} \qquad (47)$$

If M is odd, then we have:

$$\mathbf{x}(k) = \mathbf{T}_\Omega \cdot \widehat{\mathbf{A}}_\Omega^{\,k} \cdot \mathbf{T}_\Omega^{-1} \cdot \left(\mathbf{x}(0) + \mathbf{x}_1^* - \mathbf{x}_2^* + \sum_{p=1}^{M-1} \left(\mathbf{x}_{1,p}^* - \mathbf{x}_{2,p}^* \right) \right)$$
$$- \mathbf{T}_\theta \cdot \widehat{\mathbf{A}}_\theta^{\,k} \cdot \mathbf{T}_\theta^{-1} \cdot \mathbf{x}_1^* + \sum_{p=1}^{M-1} \mathbf{T}_{p \cdot \omega} \cdot \widehat{\mathbf{A}}_{p \cdot \omega}^{\,k} \cdot \mathbf{T}_{p \cdot \omega}^{-1} \cdot \left(\mathbf{x}_{2,p}^* - \mathbf{x}_{1,p}^* \right) + \mathbf{x}_2^*$$

for $k \geq 1$.

If M is even, then we have:

$$\mathbf{x}(k) = \mathbf{T}_\Omega \cdot \widehat{\mathbf{A}}_\Omega^{\,k} \cdot \mathbf{T}_\Omega^{-1} \cdot \left(\mathbf{x}(0) + \mathbf{x}_1^* - \mathbf{x}_2^* + \mathbf{x}_3^* + \sum_{\substack{p=1 \\ p \neq \frac{M}{2}}}^{M-1} \left(\mathbf{x}_{1,p}^* - \mathbf{x}_{2,p}^* \right) \right)$$
$$- \mathbf{T}_\theta \cdot \widehat{\mathbf{A}}_\theta^{\,k} \cdot \mathbf{T}_\theta^{-1} \cdot \mathbf{x}_1^* + \sum_{\substack{p=1 \\ p \neq \frac{M}{2}}}^{M-1} \mathbf{T}_{p \cdot \omega} \cdot \widehat{\mathbf{A}}_{p \cdot \omega}^{\,k} \cdot \mathbf{T}_{p \cdot \omega}^{-1} \cdot \left(\mathbf{x}_{2,p}^* - \mathbf{x}_{1,p}^* \right) + \mathbf{x}_2^*$$
$$+ (-1)^{k-1} \cdot \mathbf{x}_3^*$$

for $k \geq 1$.

Let:

$$\xi_p = \begin{bmatrix} \xi_{1,p} \\ \xi_{2,p} \end{bmatrix} = \mathbf{T}_{p \cdot \omega}^{-1} \cdot \left(\mathbf{x}_{2,p}^* - \mathbf{x}_{1,p}^* \right) \qquad (48)$$

Define the following discrete-time signals:

$$\xi_i(n) = \begin{cases} \xi_{i,-n} & -(M-1) \leq n \leq -1 \\ 0 & \text{otherwise} \end{cases} \text{ for } i = 0, 1 \qquad (49)$$

$$q_{1,k}(n) = \cos(k \cdot \omega \cdot n) \qquad (50)$$

and

$$q_{2,k}(n) = \sin(k \cdot \omega \cdot n) \qquad (51)$$

Let $Q_{1,k}(\varpi)$, $Q_{2,k}(\varpi)$, $Z_1(\varpi)$ and $Z_2(\varpi)$ be the Fourier transforms of $q_{1,k}(n)$, $q_{2,k}(n)$, $\xi_1(n)$ and $\xi_2(n)$, respectively.

If M is odd, then we have:

$$\left\{ \mathbf{x}(0) : \left\| \mathbf{T}_\Omega^{-1} \cdot \left(\mathbf{x}(0) + \mathbf{x}_1^* - \mathbf{x}_2^* + \sum_{p=1}^{M-1} \left(\mathbf{x}_{1,p}^* - \mathbf{x}_{2,p}^* \right) \right) \right\| < \right.$$
$$1 - \left\| \mathbf{T}_\theta^{-1} \cdot \mathbf{x}_1^* \right\|$$
$$\left. - \max_{k \in \{0,1,\cdots,M-1\}} \left| \frac{Z_1(k \cdot \omega) + Z_1(-k \cdot \omega)}{2} + \frac{Z_2(k \cdot \omega) - Z_2(-k \cdot \omega)}{2 \cdot j} + \frac{b_0}{1 - \cos\Omega} \right| \right\}$$
.

If M is even, then we have:

$$\left\{ \mathbf{x}(0) : \left\| \mathbf{T}_\Omega^{-1} \cdot \left(\mathbf{x}(0) + \mathbf{x}_1^* - \mathbf{x}_2^* + \mathbf{x}_3^* + \sum_{\substack{p=1 \\ p \neq \frac{M}{2}}}^{M-1} \left(\mathbf{x}_{1,p}^* - \mathbf{x}_{2,p}^* \right) \right) \right\| < \right.$$
$$1 - \left\| \mathbf{T}_\theta^{-1} \cdot \mathbf{x}_1^* \right\| -$$
$$\left. \max_{k \in \{0,1,\cdots,M-1\}} \left| \frac{Z_1'(k \cdot \omega) + Z_1'(-k \cdot \omega)}{2} + \frac{Z_2'(k \cdot \omega) - Z_2'(-k \cdot \omega)}{2 \cdot j} + \frac{b_0}{1 - \cos\Omega} - \frac{(-1)^{k-1} \cdot b_{\frac{M}{2}}}{1 + \cos\Omega} \right| \right\}$$

The proof of Lemma 10 can be found in [19].

According to Lemma 10, the set of initial conditions forms elliptical regions. If M is odd, then the centers are located at $-\mathbf{x}_1^* + \mathbf{x}_2^* - \sum_{p=1}^{M-1} \left(\mathbf{x}_{1,p}^* - \mathbf{x}_{2,p}^* \right)$ and the sizes of those ellipses depend on

$$1 - \left\| \mathbf{T}_\theta^{-1} \cdot \mathbf{x}_1^* \right\| - \max_{k \in \{0,1,\cdots,M-1\}} \left| \frac{Z_1(k \cdot \omega) + Z_1(-k \cdot \omega)}{2} + \frac{Z_2(k \cdot \omega) - Z_2(-k \cdot \omega)}{2 \cdot j} + \frac{b_0}{1 - \cos\Omega} \right|$$

. If M is even, then the centers are located at $-\mathbf{x}_1^* + \mathbf{x}_2^* - \mathbf{x}_3^* - \sum_{\substack{p=1 \\ p \neq \frac{M}{2}}}^{M-1} \left(\mathbf{x}_{1,p}^* - \mathbf{x}_{2,p}^* \right)$ and the sizes of those ellipses depend on

$$1 - \left\| \mathbf{T}_\theta^{-1} \cdot \mathbf{x}_1^* \right\| -$$
$$\max_{k \in \{0,1,\cdots,M-1\}} \left| \frac{Z_1'(k \cdot \omega) + Z_1'(-k \cdot \omega)}{2} + \frac{Z_2'(k \cdot \omega) - Z_2'(-k \cdot \omega)}{2 \cdot j} + \frac{b_0}{1 - \cos\Omega} - \frac{(-1)^{k-1} \cdot b_{\frac{M}{2}}}{1 + \cos\Omega} \right|$$

When the symbolic sequences are aperiodic, an elliptical fractal pattern or random-like chaotic pattern is found.

9. FURTHER DISCUSSIONS ON THIRD-ORDER DIGITAL FILTERS AND OTHER NONLINEARITIES

We have extended our investigations of chaotic behaviors of second-order digital filters to the third-order digital filters in cascade [17] and in parallel form [14], and we have worked out a set of necessary and sufficient conditions relating the trajectory equations, symbolic sequences and the set of initial conditions for various types of trajectories.

In most real situations, the computers and digital hardware consists of a finite number of bits. Hence, they are finite state machines, and the nonlinear function becomes a periodic quantization type function. The existing literature [5] reported that if there are more than 16 bits for the implementation, then the chaotic behaviors of the finite state machine will be visually indistinguishable from that of the infinite state machine. However, would a finite state machine behave in a near-chaotic way even when its corresponding infinite state machine does not exhibit chaotic behavior? We have found that a finite state machine may behave in a near-chaotic way even when its corresponding infinite state machine does not exhibit chaotic behavior. For more information, the readers may refer to [11].

10. CONCLUSION

In this paper, we have explored many novel and counter-intuitive results for second-order digital filters with two's complement arithmetic, and we have provided some necessary and sufficient conditions to relate the trajectory equations, symbolic sequences and the set of initial conditions for various types of trajectories. These results are useful for selecting initial conditions and designing the filter parameters so that chaotic behaviors can be avoided or generated for various applications.

11. ACKNOWLEDGMENT

12. REFERENCES

[1] L. O. Chua and T. Lin, "Chaos in digital filters," *IEEE Transactions on Circuits and Systems*, vol. 35, no. 6, pp. 648-658, June 1988.

[2] Z. Galias and M. J. Ogorzalek, "Bifurcation phenomena in second-order digital filter with saturation-type adder overflow characteristic," *IEEE Transactions on Circuits and Systems*, vol. 37, no. 8, pp. 1068-1070, August 1990.

[3] L. O. Chua and T. Lin, "Chaos and fractals from third-order digital filters," *International Journal of Circuit Theory and Applications*, vol. 18, pp. 241-255, 1990.

[4] L. O. Chua and T. Lin, "Fractal pattern of second-order non-linear digital filters: a new symbolic analysis," *International Journal of Circuit Theory and Applications*, vol. 18, pp. 541-550, 1990.

[5] T. Lin and L. O. Chua, "On chaos of digital filters in the real world," *IEEE Transactions on Circuits and Systems*, vol. 38, no. 5, pp. 557-558, May 1991.

[6] Z. Galias and M. J. Ogorzalek, "On symbolic dynamics of a chaotic second-order digital filter," *International Journal of Circuit Theory and Applications*, vol. 20, pp. 401-409, 1992.

[7] C. W. Wu and L. O. Chua, "Properties of admissible symbolic sequences in a second-order digital filter with overflow non-linearity," *International Journal of Circuit Theory and Applications*, vol. 21, pp. 299-307, 1993.

[8] L. Kocarev and L. O. Chua, "On chaos in digital filters: case b=-1," *IEEE Transactions on Circuits and Systems—II: Analog and Digital Signal Processing*, vol. 40, no. 6, pp. 404-407, June 1993.

[9] L. Kocarev, C. W. Wu and L. O. Chua, "Complex behavior in digital filters with overflow nonlinearity: analytical results," *IEEE Transactions on Circuits and Systems—II: Analog and Digital Signal Processing*, vol. 43, no. 3, pp. 234-246, March 1996.

[10] X. Yu and Z. Galias, "Periodic behaviors in a digital filter with two's complement arithmetic," *IEEE Transactions on Circuits and Systems—I: Fundamental Theory and Applications*, vol. 48, no. 10, pp. 1177-1190, October 2001.

[11] B. W. K. Ling, F. C. K. Luk and P. K. S. Tam, "Further investigation on chaos of real digital filters," to appear in *International Journal of Bifurcation and Chaos*.

[12] B. W. K. Ling and P. K. S. Tam, "Some new trajectory patterns and periodic behaviors of unstable second-order digital filter with two's complement arithmetic," to appear in *International Journal of Bifurcation and Chaos*.

[13] B. W. K. Ling, C. Y. F. Ho and P. K. S. Tam, "Detection of chaos in some local regions of phase portraits using Shannon entropies," to appear in *International Journal of Bifurcation and Chaos*.

[14] B. W. K. Ling, A. Y. P. Chan, T. P. L. Wong and P. K. S. Tam, "Autonomous response of a third-order digital filter with two's complement arithmetic realized in parallel form," to appear in *Communications in Information and Systems*.

[15] B. W. K. Ling and P. K. S. Tam, "New results on periodic symbolic sequences of second order digital filters with two's complement arithmetic," to appear in *International Journal of Circuit Theory and Applications*.

[16] B. W. K. Ling, W. F. Hung and P. K. S. Tam, "Chaotic behaviors of stable second-order digital filters with two's complement arithmetic," submitted to *International Journal of Circuit Theory and Applications*.

[17] B. W. K. Ling, W. F. Hung and P. K. S. Tam, "Autonomous response of a third-order digital filter with two's complement arithmetic realized in cascade form," submitted to *International Journal of Circuit Theory and Applications*.

[18] W. K. Ling, P. K. S. Tam and X. Yu, "Step response of a second-order digital filter with two's complement arithmetic," to appear in *IEEE Transactions on Circuits and Systems—I: Fundamental Theory and Applications*.

[19] W. K. Ling and P. K. S. Tam, "Sinusoidal response of a second-order digital filter with two's complement arithmetic," to appear in *IEEE Transactions on Circuits and Systems—I: Fundamental Theory and Applications*.

[20] B. W. K. Ling, C. Y. F. Ho and P. K. S. Tam, "Controllability, Admissibility and Invertibility of Second-order Digital Filter with Zeros and Proportional Feedback Implemented in Direct Form Using Two's Complement Arithmetic," submitted to *IEEE Transactions on Circuits and Systems—I: Fundamental Theory and Applications*.
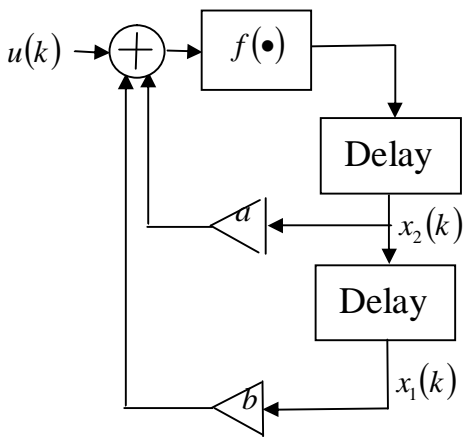
Figure 1. Insert caption to place caption below figure.
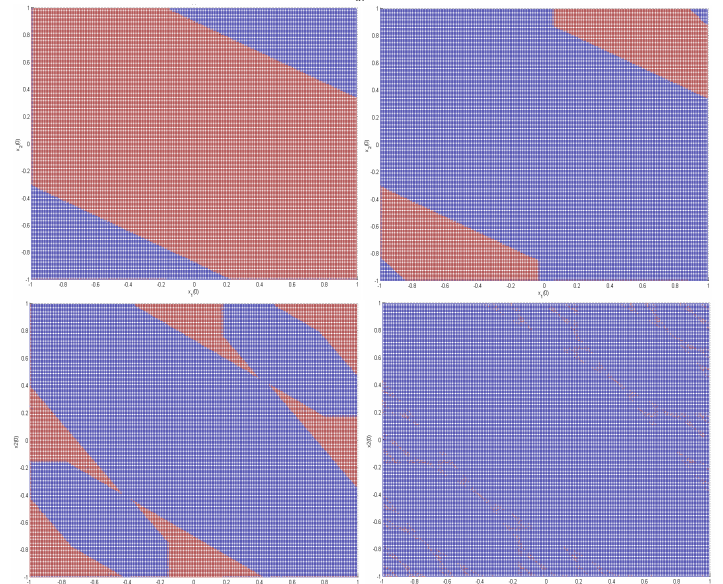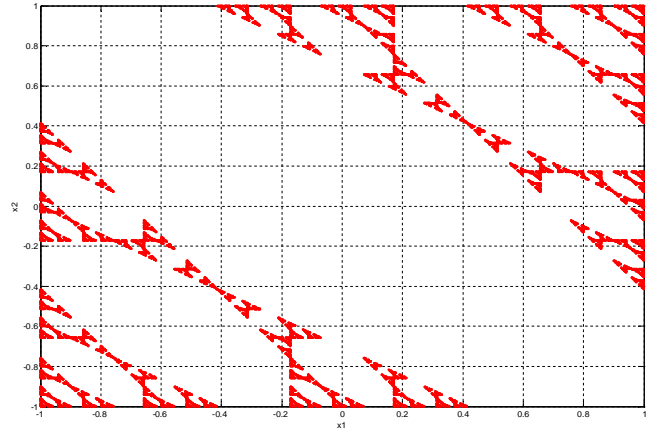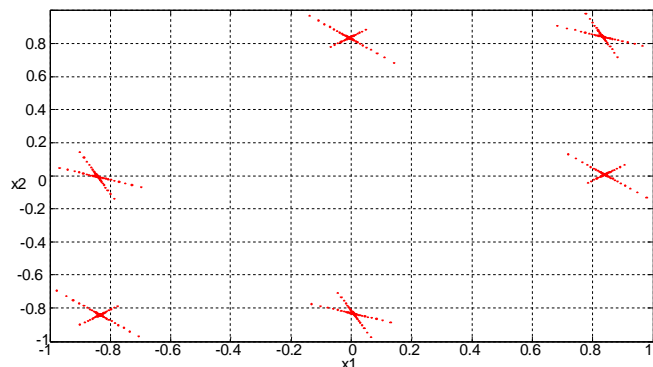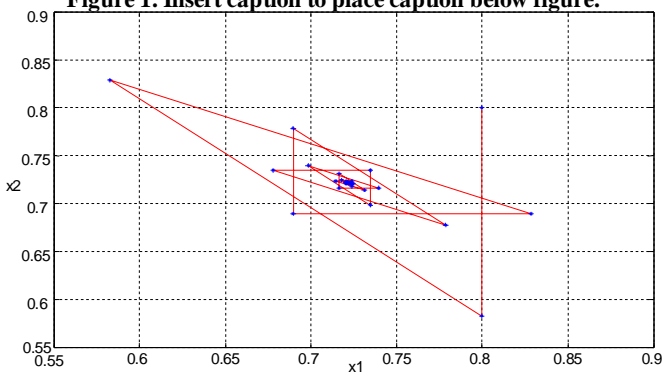
Figure 2. The phase plane (a) when the states converge to a fixed point not locating at the origin; (b) when the system exhibits limit cycle behaviors; (c) when the system exhibits chaotic fractal pattern behaviors. The set of initial conditions (d) when overflow does not occur; (e) when the symbolic sequences are constant; (f) when limit cycle occurs; (g) when chaotic fractal pattern occurs.
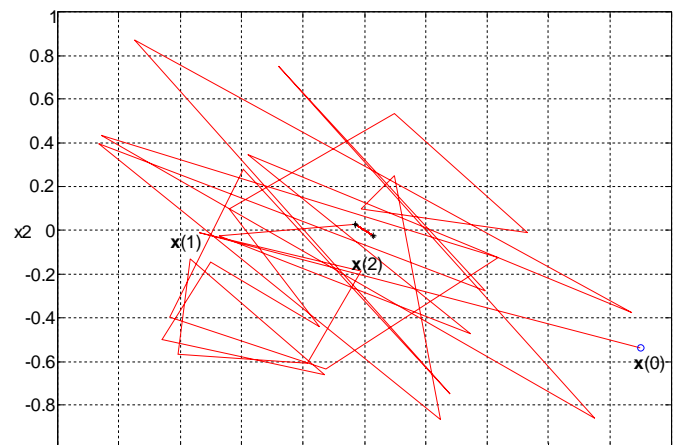
Figure 3. The phase plane of the second order digital filter with two's complement arithmetic. The points $\mathbf{x}(0)$, $\mathbf{x}(1)$, $\mathbf{x}(2)$ are as annotated, and the points with '*' denote the 'steady states' of $\mathbf{x}$.
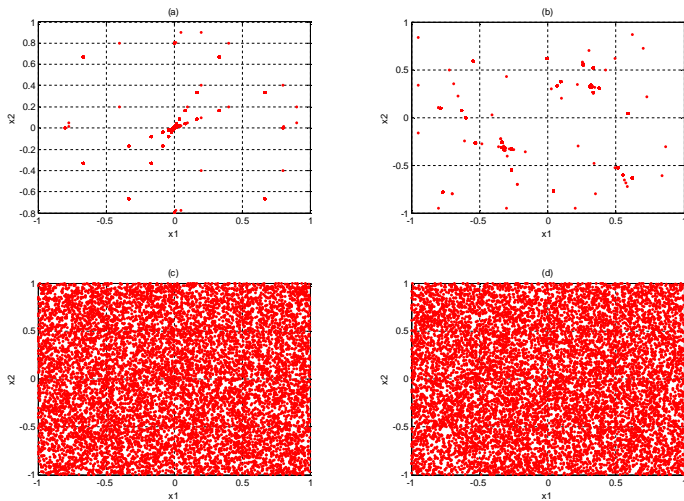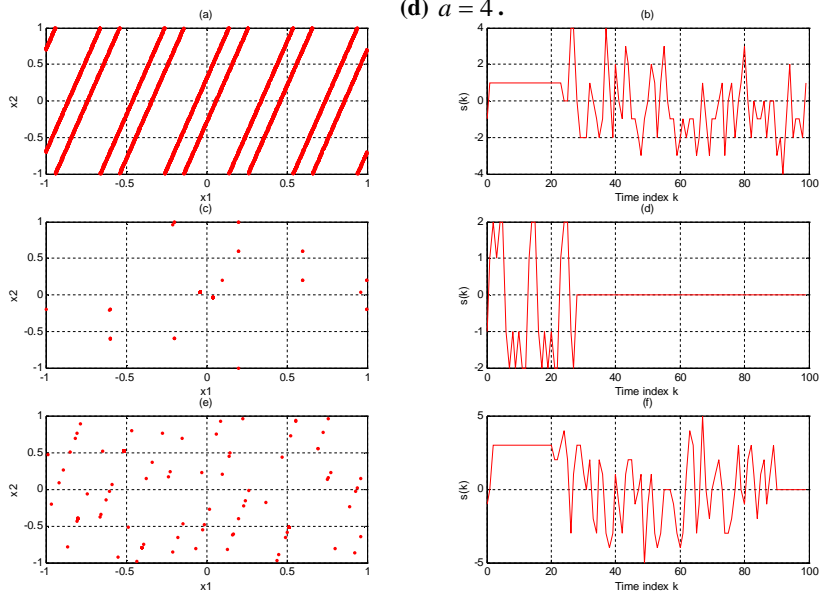
Figure 5. The phase plane and symbolic sequences with $b = a+1$, $\mathbf{x}(0) = \begin{bmatrix} 0.1 \\ 0.2 \end{bmatrix}$, and different values of a. (a) phase plane with $a = 4$, (b) symbolic sequences with $a = 4$, (c) phase plane with $a = 3$, (d) symbolic sequences with $a = 3$, (e) phase plane with $a = 5$, and (f) symbolic sequences with $a = 5$.
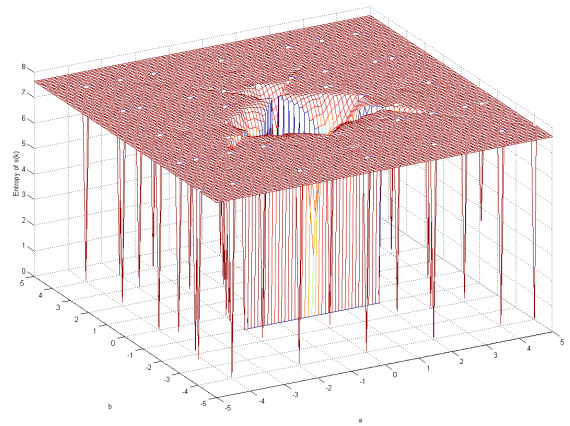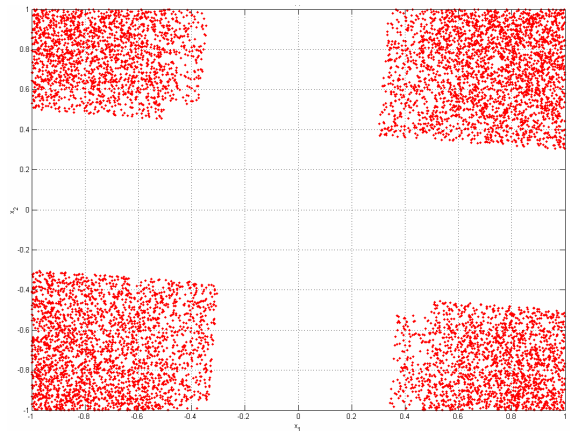

Figure 6. Shannon entropies of the state variables at different filter parameters when $\mathbf{x}(0) = \begin{bmatrix} 0.9003 \\ -0.5377 \end{bmatrix}$.
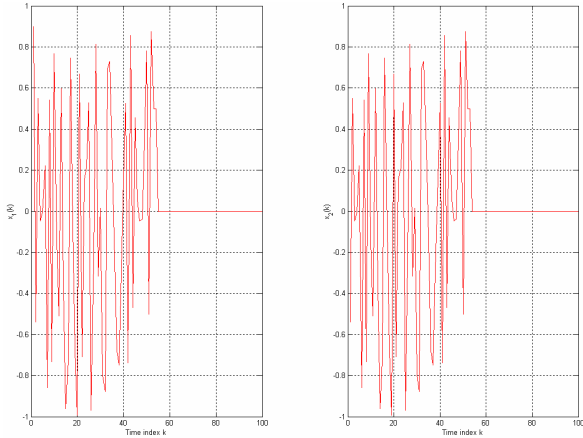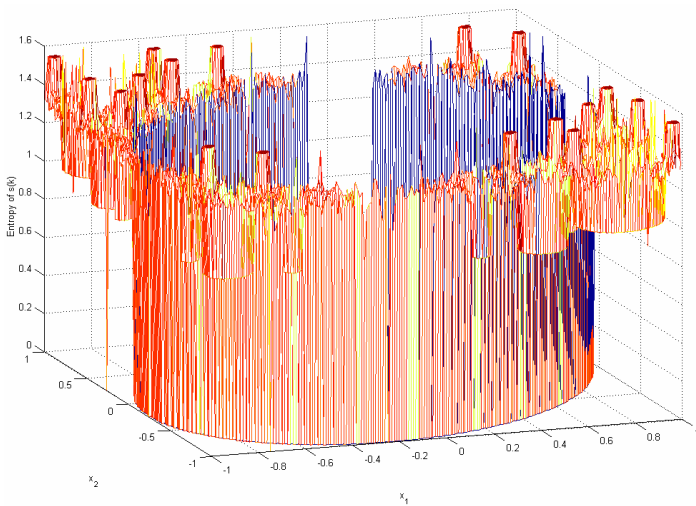
Figure 4. The phase plane with $b = -1$, $\mathbf{x}(0) = \begin{bmatrix} 0.1 \\ 0.2 \end{bmatrix}$, and different values of a. (a) $a = 2.5$, (b) $a = -4.25$, (c) $a = 3$, (d) $a = 4$.

Figure 7. (a) The phase plane of a second-order digital filter with two's complement arithmetic when $\mathbf{x}(0) = \begin{bmatrix} 0.9003 \\ -0.5377 \end{bmatrix}$, $a = -0.1$ **and** $b = -1.6$. **(b) The state trajectories of a second-order digital filter with two's complement arithmetic when**

$$\mathbf{x}(0) = \begin{bmatrix} 0.9003 \\ -0.5377 \end{bmatrix}, \; a = -4 \text{ and } b = -4.$$

Figure 8. Shannon entropies of symbolic sequences for different initial conditions when $b = -1$ **and** $a = 0.5$.

Figure 9. A phase plane and the corresponding symbolic sequence for the type III trajectory.
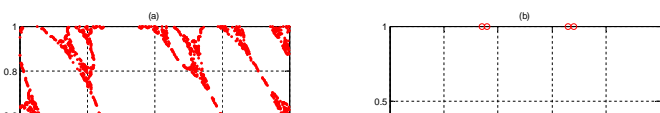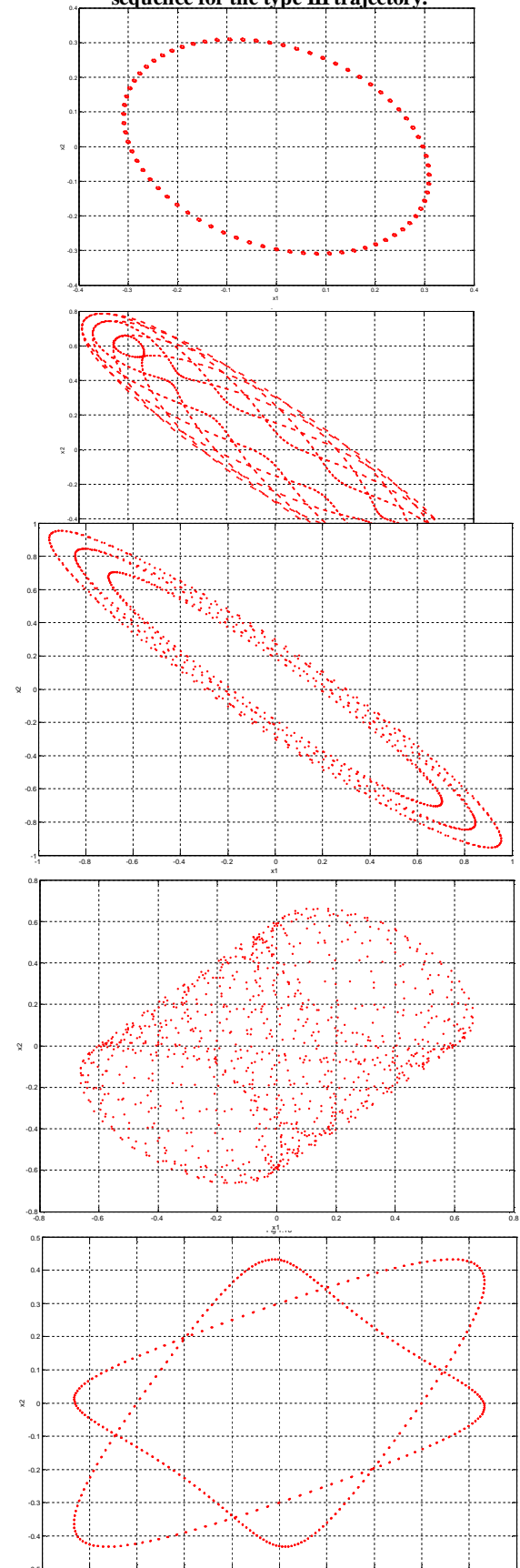
Figure 10. The phase plane of the sinusoidal response when $b=-1$, $\mathbf{x}(0)=\begin{bmatrix} 0.3 \\ 0 \end{bmatrix}$, **and different values of** c, θ **and** Ω.